



Article

Mobility Enhancement in Amorphous In-Ga-Zn-O Thin-Film Transistor by Induced Metallic In Nanoparticles and Cu Electrodes

Shiben Hu ¹ , Honglong Ning ^{1,*} , Kuankuan Lu ¹, Zhiqiang Fang ¹ , Yuzhi Li ¹,
Rihui Yao ^{1,*} , Miao Xu ¹, Lei Wang ¹, Junbiao Peng ¹ and Xubing Lu ²

¹ Institute of Polymer Optoelectronic Materials and Devices, State Key Laboratory of Luminescent Materials and Devices, South China University of Technology, Guangzhou 510640, China; hushiben@foxmail.com (S.H.); kk-lu@foxmail.com (K.L.); fangzq1230@126.com (Z.F.); liyuzhi1991@foxmail.com (Y.L.); xumiao4049@126.com (M.X.); mslwang@scut.edu.cn (L.W.); psjbpeng@scut.edu.cn (J.P.)

² Institute for Advanced Materials, Guangdong Provincial Key Laboratory of Quantum Engineering and Quantum Materials, South China Normal University, Guangzhou 510006, China; luxubing@m.scnu.edu.cn

* Correspondence: ninghl@scut.edu.cn (H.N.); yaorihui@scut.edu.cn (R.Y.)

Received: 6 February 2018; Accepted: 25 March 2018; Published: 27 March 2018



Abstract: In this work, we fabricated a high-mobility amorphous indium-gallium-zinc-oxide (a-IGZO) thin-film transistor (TFT) based on alumina oxide (Al₂O₃) passivation layer (PVL) and copper (Cu) source/drain electrodes (S/D). The mechanism of the high mobility for a-IGZO TFT was proposed and experimentally demonstrated. The conductivity of the channel layer was significantly improved due to the formation of metallic In nanoparticles on the back channel during Al₂O₃ PVL sputtering. In addition, Ar atmosphere annealing induced the Schottky contact formation between the Cu S/D and the channel layer caused by Cu diffusion. In conjunction with high conductivity channel and Schottky contact, the a-IGZO TFT based on Cu S/D and Al₂O₃ PVL exhibited remarkable mobility of 33.5–220.1 cm²/Vs when channel length varies from 60 to 560 μm. This work presents a feasible way to implement high mobility and Cu electrodes in a-IGZO TFT, simultaneously.

Keywords: IGZO; thin film transistors; indium; copper; Schottky contact

1. Introduction

As display technology advances in terms of size, resolution and refresh rate, a high mobility thin film transistor (TFT) array with low resistivity interconnection lines is required to decrease resistance–capacitance delay to avoid signal distortions [1,2]. Amorphous oxide semiconductor (AOS) TFTs have attracted considerable attention on the flat panel display backplanes because of their high mobility and excellent uniformity [3]. On the other hand, a low resistivity metal line is required to meet the stringent demand for high resolution (≥UHD), large panel size (≥80 inch) and high refresh rate (≥240 Hz) [4–6]. In this regard, copper (Cu) is an appropriate electrode material for its lower resistivity than aluminum (Al) [7,8]. However, Cu atoms tend to diffuse into metal oxide semiconductors as acceptors or acceptor-like traps [9,10] during thermal annealing, resulting in degradation of electrical properties. This effect limits its application in TFT array backplanes as source/drain electrodes (S/D) that involve direct contact with AOS.

However, in this paper, Cu S/D play an important role in the performance of amorphous indium-gallium-zinc oxide (a-IGZO) TFTs. In one aspect, Al₂O₃ passivation layer (PVL)-induced metallic indium nanoparticles significantly improved the conductivity of the a-IGZO channel layer. On the other hand, Cu S/D formed Schottky contact with the channel layer after being annealed

in an Ar atmosphere, which was advantageous for the a-IGZO TFT to achieve typical switching characteristics. Through these two effects, the a-IGZO TFT achieved mobility of up to 220.7 cm²/Vs.

2. Results and Discussion

We prepared three kinds of a-IGZO TFTs, including non-passivated Cu-contact device, passivated Mo-contact device and passivated Cu-contact device. Before the post-annealing process, the three devices were labeled as S1, S3, and S4. After the post-annealing process, they were marked as S2, S5, and S6. Figure 1 shows the representatives' output and transfer curves of the above six TFTs. Moreover, the electrical performance of the six TFTs is summarized in Table 1. In this case, the field effect mobility (μ_{FE}) and the threshold voltage (V_{th}) were extracted through the curve of the square root of the drain current ($I_D^{1/2}$) versus the gate voltage (V_G) in saturated operation region using the following equation:

$$I_D^{1/2} = \left(\frac{WC_i\mu_{FE}}{2L} \right)^{1/2} (V_G - V_{th}).$$

Here, W and L are channel width and length, respectively. C_i is the gate capacitance per unit area of the insulator layer. Moreover, the subthreshold swing (SS) was extracted as the inverse of the maximum slope of the curve of $\text{Log } I_D$ versus the V_G [11]:

$$SS = \left[\left(\frac{d \text{Log } I_D}{dV_G} \right)_{max} \right]^{-1}.$$

The S2 device that suffered post-annealing treatment exhibited a degraded performance compared with the S1 device. It is a common phenomenon in many reports due to the diffusion of Cu caused by the thermal treatment [12]. It is obvious that the drain current of the S3–S5 devices could not be modulated by gate voltage (V_G). These samples showed conductor behavior with an almost constant current versus gate voltage swept. The maximum drain current of the S3–S6 devices significantly increased compared with the S1 and S2 devices that have no Al₂O₃ PVL. This phenomenon indicates a high conductivity a-IGZO channel formed by the deposition of Al₂O₃ PVL. Compared to the S1–S5 devices, the S6 device showed a μ_{FE} of 220.7 cm²/Vs, a V_{th} of 5.7 V, an SS of 0.78 V/dec and an I_{on}/I_{off} of 1.1×10^8 . Therefore, we can attribute the high performance of the S6 device to the Al₂O₃ PVL and Cu S/D.

Table 1. Device performance for both a-IGZO TFTs

Sample	S/D	Al ₂ O ₃ PVL	Post-Annealing	V_{th} (V)	μ_{FE} (cm ² /Vs)	SS (V/dec)	I_{on}/I_{off}
S1	Cu	No	No	3.5	8.2	0.26	3.3×10^7
S2	Cu	No	Yes	10.0	6.8	0.43	9.2×10^6
S3	Mo	Yes	No	—	—	—	—
S4	Cu	Yes	No	—	—	—	—
S5	Mo	Yes	Yes	—	—	—	—
S6	Cu	Yes	Yes	5.7	220.7	0.78	1.1×10^8

For evaluating the effect of Al₂O₃ PVL and Cu S/D, a transmission line method (TLM) [13] was utilized to trace the variation of the channel and contact resistance using the TFT with different channel length. The total resistance (R_T) was defined as the sum of channel resistance and contact resistance by the following equation at $V_D = 0.1$ V:

$$R_T = \frac{V_D}{I_D} = r_{ch}L + R_C,$$

where r_{ch} is the channel resistance per unit channel length, and R_C is the total contact resistance. Figure 2 exhibits the variation of R_C and r_{ch} versus gate voltage before and after the post-annealing process. It is observed that the r_{ch} of the S3–S6 devices that were passivated by Al₂O₃ films significantly

decreased compared with the S1 and S2 devices. This phenomenon indicates that the sputtering of Al₂O₃ PVL can dramatically reduce the channel resistance in a-IGZO TFTs. For contact resistance evolution, the R_C of the S2 and S6 devices significantly increased after post-annealed treatment. This increase is consistent with the previous report that Cu diffusion leads to a decrease in carrier concentration at the contact area [14]. Finally, we found that the S5 device has the similar r_{ch} and lower R_C as the S6 device. However, the S5 device behaved like a conductor, and the S6 device exhibited typical switching characteristics. According to their electrical properties, we can infer that high contact resistance caused by Cu diffusion and low channel resistance due to Al₂O₃ sputtering should be responsible for the high performance of the S6 device.

Figure 3 shows the dependence characteristics of the channel length on the apparent field-effect mobility (μ_{app}) of the a-IGZO TFTs. As the channel length decreased from 560 μm to 60 μm , the μ_{app} dropped from 220.1 cm^2/Vs to 33.5 cm^2/Vs . This decrease should be due to the reduction of the drain voltage drop as channel length reduces. Therefore, we used the following equation to exclude the influence of the contact resistance to extract the intrinsic mobility of the TFTs [15]:

$$\mu_{app} = \mu_{ins} \frac{1}{1 + R_C \frac{W}{L} C_i \mu_{ins} (V_G - V_T)},$$

where μ_{ins} is the intrinsic mobility and μ_{app} is the apparent field-effect mobility extracted in the linear regime of I_D - V_G curves at $V_D = 0.1$ V. The equation was used to fit the experimental results in Figure 3. A good agreement between the experimental results and the fitting was achieved. The extracted value of the μ_{ins} was 675.8 cm^2/Vs .

High-resolution transmission electron microscopy (HR-TEM) integrated with X-ray energy dispersive spectroscopy (EDS) was performed to clarify the interface reaction of Al₂O₃ PVL with the a-IGZO channel layer. Figure 4a shows a cross-sectional HR-TEM image of the S5 device channel, while Figure 4b,c shows a magnified image taken from Figure 4a. The interfacial morphology between Al₂O₃ PVL and the a-IGZO film was clearly observed. We note that a thin layer formed at the interface was most likely induced by the sputtering of Al₂O₃ PVL. Figure 4d shows the corresponding chemical composition of the particle comprising In, Al and O. The HR-TEM image illustrated in Figure 4e indicated a single-crystalline feature where the internal plane spacing of 0.230 nm, 0.279 nm and 0.176 nm were indexed, which matched with the (110), (101) and (112) planes of metallic indium, respectively. Based on the above results, it is entirely reasonable to assume that the bombardment of energetic particles dissociates oxygen in indium oxide during the sputtering of Al₂O₃ PVL to form metallic indium nanoparticles. Moreover, these indium nanoparticles can increase carrier concentration and act as conduction paths to lower the channel resistance. However, as the carrier concentration in the channel increased, the depletion layer capacitance also increased, which resulted in a larger SS than the device without the Al₂O₃ PVL [16].

Current-voltage (I-V) characteristics of the a-IGZO films with different metal electrodes were used to investigate contact properties. Figure 5 shows the I-V characteristics of a-IGZO films with Cu and Mo S/D. As shown in the figure, the Mo-contact film showed perfect ohmic contact with linear curves. Moreover, the Cu-contact film exhibited regular Schottky contact. It is widely known that Cu doping is introduced as acceptors or acceptor-like traps in ZnO [17] and InGaZnO_x [18] films to suppress the carrier concentration because the chemical bonds of Cu-O form a covalent hybridized band between the O 2p and Cu 3d orbitals at the top of the valence band, resulting in p-type properties [19]. In this case, a decrease in the carrier concentration beneath the contact area due to Cu diffusion results in a high contact potential, which makes the Cu-contact device behave like a Schottky contact. From these results, the operating mechanism of the high mobility TFT can be attributed to the formation of the Schottky contact. As mentioned by previous researchers [20,21], the Schottky contact induces a high barrier at both ends of the S and D electrodes, which prevents the electrons from passing freely through the channel at a high negative gate voltage, thereby suppressing the leakage current of the TFT, even if the active layer is highly conductive. Thus, the TFT can be switched on/off normally.

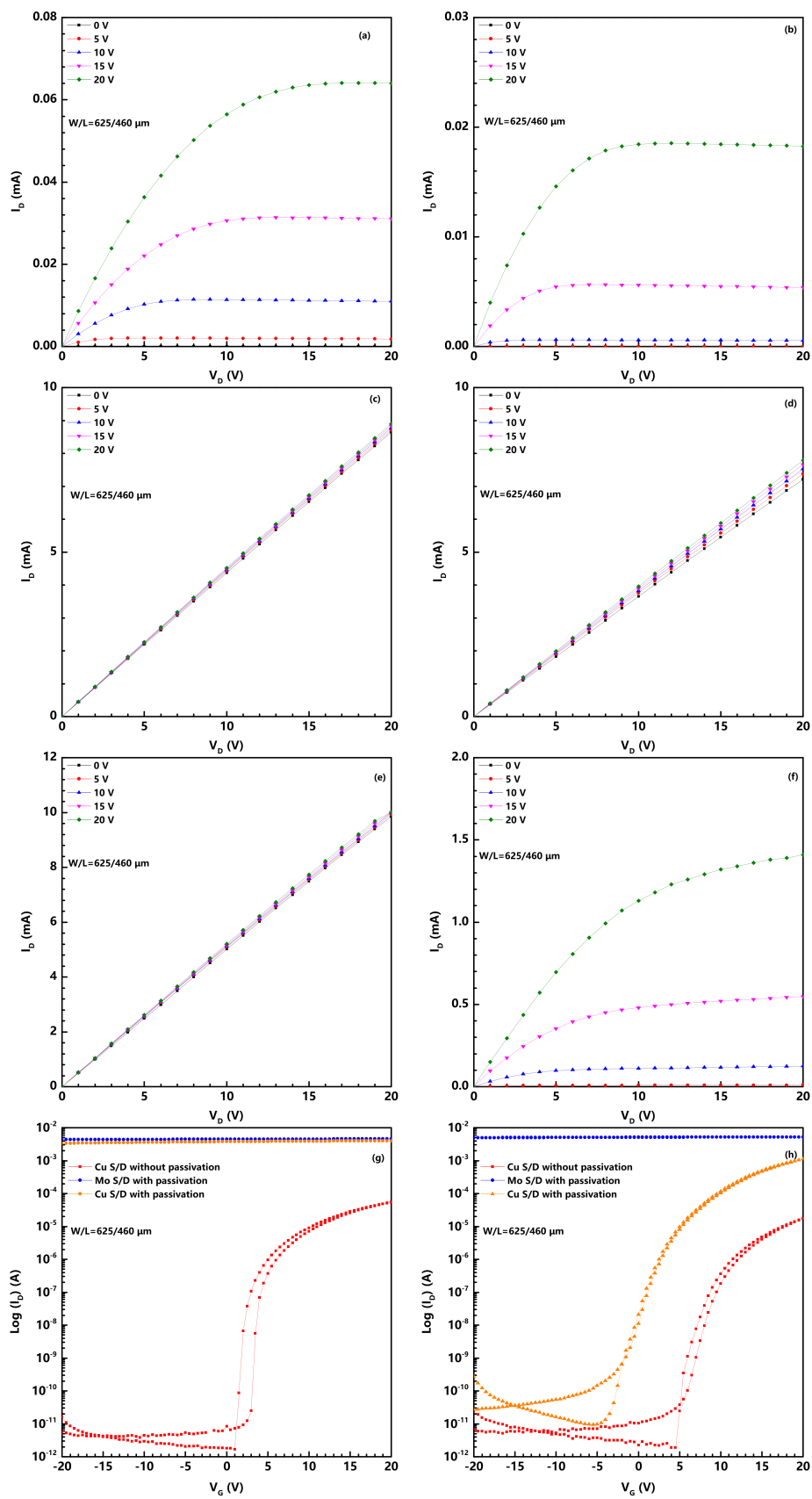


Figure 1. (a–f) output characteristics for S1, S2, S3, S4, S5 and S6 devices, respectively; transfer curves of a-IGZO TFTs (g) before post-annealing and (h) after post-annealing measured at drain voltage (V_D) equal to 10.1 V.

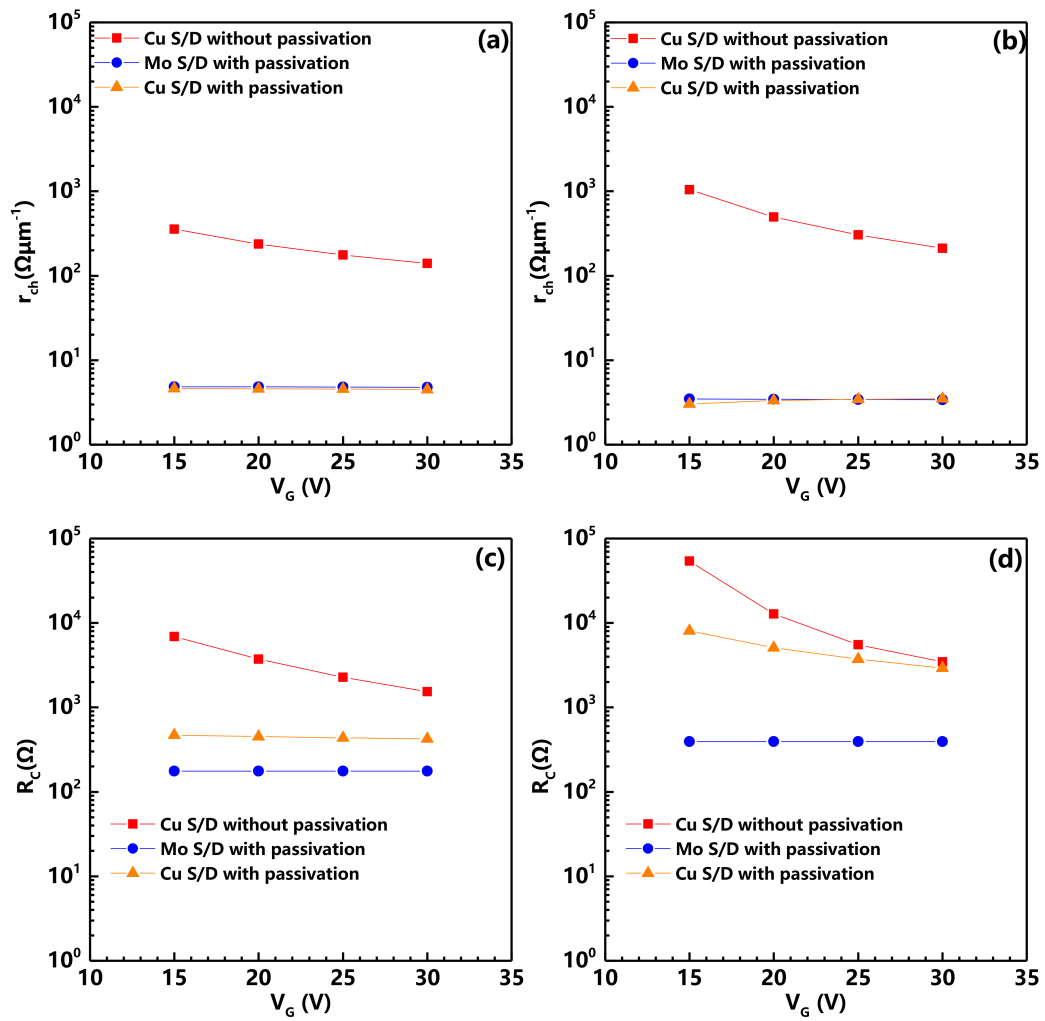


Figure 2. Channel resistance per unit channel length (r_{ch}) for a-IGZO TFTs (a) before post-annealing and (b) after post-annealing, and contact resistance (R_C) for a-IGZO TFTs (c) before post-annealing and (d) after post-annealing as a function of V_G .

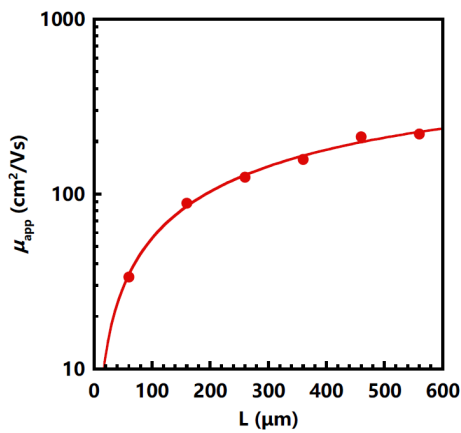


Figure 3. The extracted apparent field-effect mobility μ_{app} as a function of channel length and the fitting result considering the contact resistance.

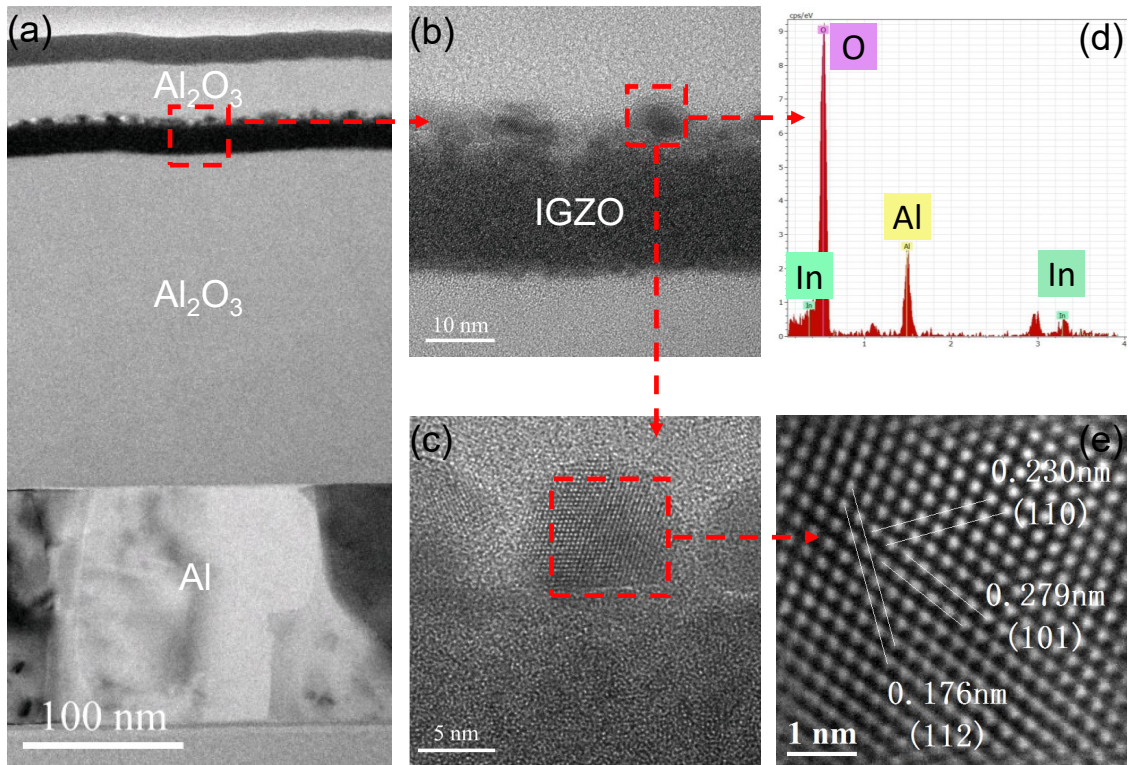


Figure 4. (a) cross-sectional image of a-IGZO TFT with Cu S/D and Al₂O₃ PVL; the (b) 450 k and (c) 910 k magnified image of the interface between a-IGZO and Al₂O₃ PVL; (d) corresponding EDS and (e) HR-TEM image of the particles.

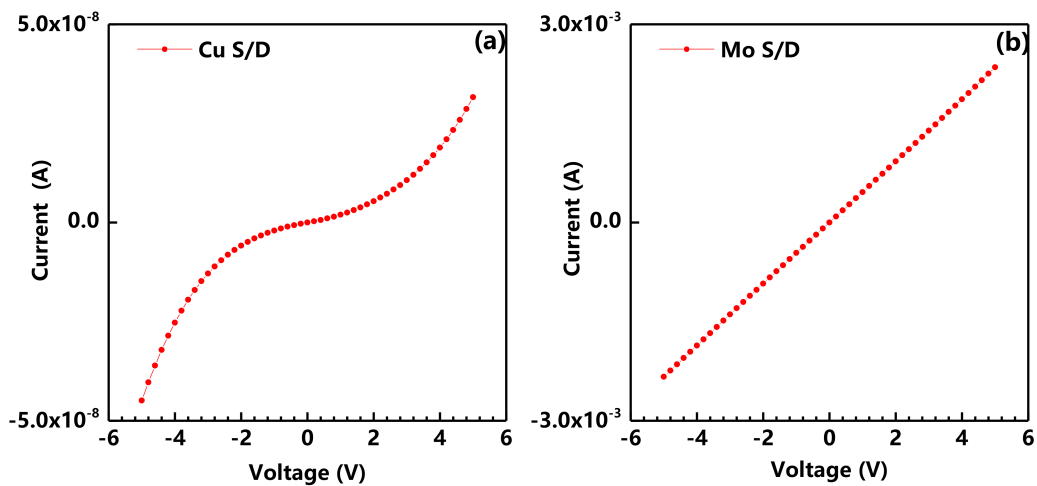


Figure 5. Current-Voltage (I-V) characteristics of a-IGZO film with different metal electrodes Cu S/D (a) and Mo S/D (b).

The electrical stability of the S6 device under gate bias stress ($V_G = 10$ V for positive bias stress (PBS) and -10 V for negative bias stress (NBS), V_D fixed at 10 V) is also investigated, as shown in Figure 6. It is clearly observed that the TFT exhibits excellent electrical stability with the V_{th} shift of only 0.6 V for PBS and -0.2 V for NBS, indicating that the Al₂O₃ PVL can effectively protect the TFT from the ambient influence.

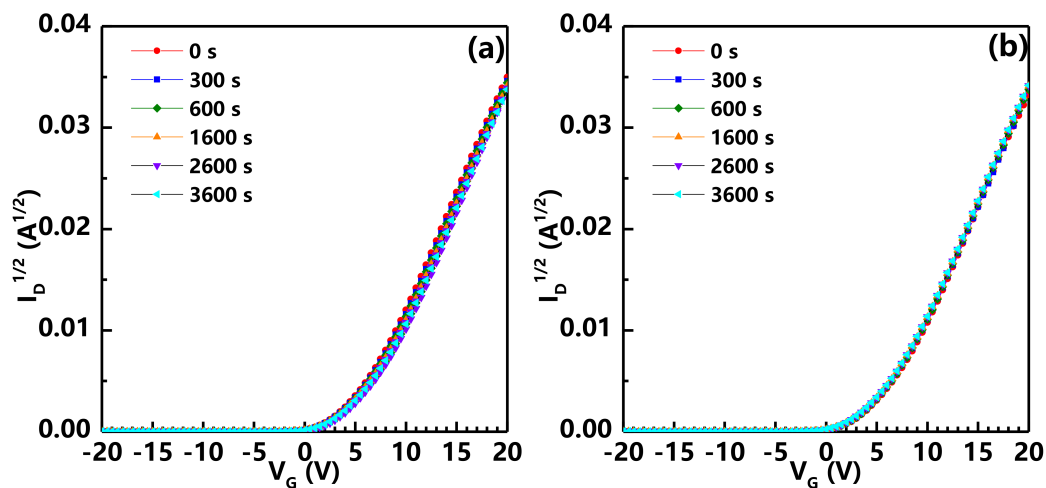


Figure 6. Variations of the transfer characteristics of a-IGZO TFT with Cu S/D and Al₂O₃ PVL after post-annealing under (a) positive and (b) negative bias stress for 3600 s.

3. Materials and Methods

A bottom-gate, top-contact configuration was used in the a-IGZO TFTs. Firstly, an Al gate electrode was deposited on the glass with a thickness of 300 nm. Then, an anodic Al₂O₃ gate insulator layer having a thickness of 190 nm was formed on the surface of the gate electrode by an anodic oxidation process. Details of the anodic oxidation technology have ever been reported elsewhere [22]. Then, a 25 nm thick a-IGZO (In:Ga:Zn = 1:1:1) film was deposited by radio frequency (RF) magnetron sputtering and patterned through a metal shadow mask. After that, the a-IGZO thin film was pre-annealed at 450 °C for 1 h in the air. Cu or Mo thin films (200 nm of thickness), as source and drain electrodes (S/D), were deposited on an a-IGZO layer by direct current (DC) magnetron sputtering and patterned using a shadow mask. After that, a 30-nm thick Al₂O₃ thin film, as a passivation layer (PVL), was formed by RF magnetron sputtering using an Al₂O₃ target. Finally, a post-annealed treatment was carried out in an argon atmosphere at 350 °C for 1 h.

The cross-sectional properties of each functional film were characterized by transmission electron microscopy (TEM, FEI HELIOS NANOLAB 450s, Hillsboro, OR, USA) equipped with an X-ray energy-dispersive spectroscopy (EDS). The electrical characterization was conducted by a semiconductor parameter analyzer (Agilent 4155C, Santa Clara, CA, USA) in the air.

4. Conclusions

In summary, we successfully fabricated a high-performance a-IGZO TFT based on Cu S/D with Al₂O₃ PVL. According to the TEM/EDS analyses, it is found that an In-rich layer formed after the sputtering of Al₂O₃ PVL. The conductive In nanoparticles in the In-rich layer serve as conduction paths to accelerate the carrier transport. Moreover, a Schottky contact created at the Cu S/D and a-IGZO channel interfaces due to Cu diffusion caused by the post-annealing treatment. Thus, the TFT with long channel length exhibited good switching operations and a high mobility exceeding 200 cm²/Vs. Moreover, the TFT also showed superior positive and negative gate bias stress stability.

Acknowledgments: This work was supported by the National Key R&D Program of China (No. 2016YFB0401504), the National Natural Science Foundation of China (No. 51771074 and U1601651), the National Key Basic Research and Development Program of China (973 program, No. 2015CB655004) founded by Ministry of Science and Technology, the Guangdong Natural Science Foundation (No. 2016A030313459 and 2017A030310028), the Science and Technology Project of Guangdong Province (No. 2016B090907001, 2016A040403037 and 2016B090906002), and the Project for Guangdong Province Universities and Colleges Pearl River Scholar Funded Scheme (2016).

Author Contributions: S.H., H.N., and R.Y. conceived and designed the experiments; S.H. performed the experiments; S.H., H.N., and R.Y. analyzed the data; K.L., Z.F., Y.L., R.Y., M.X., L.W., J.P., and X.L. contributed reagents/materials/analysis tools; and S.H., H.N., Y.L. and R.Y. wrote the paper.

Conflicts of Interest: The authors declare no conflict of interest.

References

1. Liao, Y.; Shao, X.; Du, Y.; Song, Y.; Hu, W.; Zhang, Z.; Chen, Y.; Wang, Y.; Ma, Q.; Yoon, D.; et al. Development of a 120 Hz 110" ultra-high-definition a-Si liquid crystal display panel. *J. Inf. Disp.* **2014**, *15*, 77–80.
2. Gong, N.; Park, C.; Lee, J.; Jeong, I.; Han, H.; Hwang, J.; Park, J.; Park, K.; Jeong, H.; Ha, Y.; et al. 58.2: Distinguished Paper: Implementation of 240 Hz 55-inch Ultra Definition LCD Driven by a-IGZO Semiconductor TFT with Copper Signal Lines. *SID Symp. Digest Tech. Pap.* **2012**, *43*, 784–787.
3. Nomura, K.; Ohta, H.; Takagi, A.; Kamiya, T.; Hirano, M.; Hosono, H. Room-temperature fabrication of transparent flexible thin-film transistors using amorphous oxide semiconductors. *Nature* **2004**, *432*, 488–492.
4. Zhou, L.; Xu, M.; Xia, X.H.; Zou, J.H.; Zhang, L.R.; Luo, D.X.; Wu, W.J.; Wang, L.; Peng, J.B. Power Consumption Model for AMOLED Display Panel Based on 2T-1C Pixel Circuit. *J. Disp. Technol.* **2016**, *12*, 1064–1069.
5. Zhao, M.; Xu, M.; Ning, H.; Xu, R.; Zou, J.; Tao, H.; Wang, L.; Peng, J. Method for Fabricating Amorphous Indium-Zinc-Oxide Thin-Film Transistors With Copper Source and Drain Electrodes. *IEEE Electron Device Lett.* **2015**, *36*, 342–344.
6. Hu, S.; Fang, Z.; Ning, H.; Tao, R.; Liu, X.; Zeng, Y.; Yao, R.; Huang, F.; Li, Z.; Xu, M.; Wang, L.; Lan, L.; Peng, J. Effect of Post Treatment For Cu-Cr Source/Drain Electrodes on a-IGZO TFTs. *Materials* **2016**, *9*, 623.
7. Kim, W.S.; Moon, Y.K.; Lee, S.; Kang, B.W.; Kwon, T.S.; Kim, K.T.; Park, J.W. Copper source/drain electrode contact resistance effects in amorphous indium-gallium-zinc-oxide thin film transistors. *Phys. Status Solidi Rapid Res. Lett.* **2009**, *3*, 239–241.
8. Lee, C.K.; Park, S.Y.; Jung, H.Y.; Lee, C.K.; Son, B.G.; Kim, H.J.; Lee, Y.J.; Joo, Y.C.; Jeong, J.K. High performance Zn-Sn-O thin film transistors with Cu source/drain electrode. *Phys. Status Solidi Rapid Res. Lett.* **2013**, *7*, 196–198.
9. Ka, J.; Cho, E.N.; Lee, M.J.; Myoung, J.M.; Yun, I. Electrode metal penetration of amorphous indium gallium zinc oxide semiconductor thin film transistors. *Curr. Appl. Phys.* **2015**, *15*, 675–678.
10. Tai, Y.H.; Chiu, H.L.; Chou, L.S. The deterioration of a-IGZO TFTs owing to the copper diffusion after the process of the source/drain metal formation. *J. Electrochem. Soc.* **2012**, *159*, J200–J203.
11. Fortunato, E.; Barquinha, P.; Martins, R. Oxide Semiconductor Thin-Film Transistors: A Review of Recent Advances. *Adv. Mater.* **2012**, *24*, 2945–2986.
12. Yim, J.R.; Jung, S.Y.; Yeon, H.W.; Kwon, J.Y.; Lee, Y.J.; Lee, J.H.; Joo, Y.C. Effects of metal electrode on the electrical performance of amorphous In–Ga–Zn–O thin film transistor. *Jpn. J. Appl. Phys.* **2011**, *51*, 011401.
13. Jaechul, P.; Changjung, K.; Sunil, K.; Ihun, S.; Sangwook, K.; Donghun, K.; Hyuck, L.; Huaxiang, Y.; Ranju, J.; Eunha, L.; et al. Source/drain series-resistance effects in amorphous gallium-indium zinc-oxide thin film transistors. *IEEE Electron Device Lett.* **2008**, *29*, 879–881.
14. Kim, W.S.; Moon, Y.K.; Kim, K.T.; Lee, J.H.; Ahn, B.D.; Park, J.W. An investigation of contact resistance between metal electrodes and amorphous gallium-indium-zinc oxide (a-GIZO) thin-film transistors. *Thin Solid Films* **2010**, *518*, 6357–6360.
15. Uemura, T.; Rolin, C.; Ke, T.; Fesenko, P.; Genoe, J.; Heremans, P.; Takeya, J. On the Extraction of Charge Carrier Mobility in High-Mobility Organic Transistors. *Adv. Mater.* **2016**, *28*, 151.
16. Brotherton, S.D. *Introduction to Thin Film Transistors*; Springer Verlag: Berlin, Germany, 2013.
17. Kanai, Y. Admittance spectroscopy of Cu-doped ZnO crystals. *Jpn. J. Appl. Phys.* **1991**, *30*, 703–707.
18. Kim, S.I.; Park, J.S.; Kim, C.J.; Park, J.C.; Song, I.; Park, Y.S. High Reliable and Manufacturable Gallium Indium Zinc Oxide Thin-Film Transistors Using the Double Layers as an Active Layer. *J. Electrochem. Soc.* **2009**, *156*, H184.
19. Nandy, S.; Banerjee, A.; Fortunato, E.; Martins, R. A Review on Cu₂O and Cu^I-Based p-Type Semiconducting Transparent Oxide Materials: Promising Candidates for New Generation Oxide Based Electronics. *Rev. Adv. Sci. Eng.* **2013**, *2*, 273–304.
20. Trinh, T.T.; Jang, K.; Dao, V.A.; Yi, J. Effect of high conductivity amorphous InGaZnO active layer on the field effect mobility improvement of thin film transistors. *J. Appl. Phys.* **2014**, *116*, 214504.

21. Trinh, T.T.; Jang, K.; Velumani, S.; Dao, V.A.; Yi, J. Role of Schottky barrier height at source/drain contact for electrical improvement in high carrier concentration amorphous InGaZnO thin film transistors. *Mater. Sci. Semicond. Process.* **2015**, *38*, 50–56.
22. Luo, D.; Lan, L.; Xu, M.; Xu, H.; Li, M.; Wang, L.; Peng, J. Role of Rare Earth Ions in Anodic Gate Dielectrics for Indium-Zinc-Oxide Thin-Film Transistors. *J. Electrochem. Soc.* **2012**, *159*, H502.



© 2018 by the authors. Licensee MDPI, Basel, Switzerland. This article is an open access article distributed under the terms and conditions of the Creative Commons Attribution (CC BY) license (<http://creativecommons.org/licenses/by/4.0/>).